CYCLIC TESTS OF VERTICALLY-CORRUGATED STEEL PLATE SHEAR WALLS WITH VARIOUS OPENINGS

J. Qiu [(1)], Q.H. Zhao [(2)]
[(1)] *PhD candidate, School of Civil Engineering, Tianjin University, jqiu@tju.edu.cn*
[(2)] *Professor, School of Civil Engineering, Tianjin University; Key Laboratory of Coast Civil Structure and Safety of China Ministry of Education, qzhao@tju.edu.cn*

Abstract

Vertically corrugated steel plate shear wall is a new type of lateral load-resisting system suitable for mid- to high-rise buildings, which has the advantages of superior seismic performance, simple construction, fulfillment of architectural function, and convenient adjustment of structural performance. Four 1/3 scale two-story single-bay vertically corrugated steel plate shear walls with various infill panels (panel without opening, panel with bilateral gaps, panel with bilateral openings, and panel with central opening) were tested under cyclic lateral loads. Failure mode, cyclic behavior, strength and stiffness properties, deformation and energy dissipation capacities of the specimens were presented and discussed. Influences of opening size, opening location and end plates at the free edges on the seismic behavior were studied. Test results shown that all specimens exhibited excellent seismic performance, with high lateral stiffness and capacity, stable cyclic post-buckling performance, and ductility in the range of 4.67 to 6.12. Compared with the specimen with no opening, the lateral capacity of the specimen with bilateral gaps, the specimen with bilateral openings and the specimen with central opening were reduced by 13%, 26%, 14% respectively, and the lateral stiffness were reduced by 20%, 27%, 33% respectively. With the same opening ratio, the lateral stiffness of the specimen with bilateral openings was 8% lower than the specimen with central opening, but with higher capacity and ductility, which might be mainly due to the immature beam-column connections failure in the former specimen. Welding end plates to the free edges of corrugated wall panels improved the load-carrying efficiency evidently. Recommendations on seismic design of vertically-corrugated steel plate shear walls connected with beams only were also proposed.

Keywords: corrugated steel plate shear wall; wall panels connected with beams only; hysteretic behavior; yielding mechanism

1. Introduction

Steel plate shear wall (SPSW), which is composed of a boundary frame and infill steel wall panels, has been proved to be an effective lateral load-resisting system in high intensity area, due to its high lateral stiffness, lateral strength, ductility, redundancy, and energy consumption capacity [1]. However, conventional flat wall panels tend to buckle elastically under low levels of lateral loads or gravity loads, this would lead to considerable reduction of lateral stiffness and capacity [2]. In addition, pull-in forces from infill wall panels acting on the columns would cause considerable bending moments and axial forces in the column, which would lead to very large column sections for conventional SPSWs [3].

Corrugated steel plate shear walls (CPSWs), in which corrugated plates are applied as the wall panels instead of flat panels to greatly improve the buckling performance of the wall plate through special geometric form [4-6], were proposed to provide a more effective lateral-resisting system. In addition, corrugated wall panel can effectively alleviate the construction delay caused by the buckling of conventional flat panel under vertical loads, which is very beneficial for high-rise building projects [7]. Several large-scale tests and numerical research have been shown that the CPSW possesses high level of initial stiffness, ductility and energy consumption capacity [4-9]. It has also been pointed out that the parameters of corrugated section have a great influence on the seismic performance of CPSWs, and lateral load-resisting mechanism of corrugated wall panels could range from shear yielding to different levels of inelastic shear buckling, which was different from tensioned field action (TFA) mechanism of flat wall panels [7]. CPSWs with wall panels with high buckling stability, of which the corrugated section was reasonably designed, have excellent seismic performance, including high lateral stiffness, bearing capacity, ductility and energy consumption capacity [10,11]. For the design of corrugated section parameters, researchers studied the effects of various parameters on the buckling performance of corrugated wall panels and gave some reasonable design suggestions for the corrugated wall panels to make the CPSW have good seismic performance [12,13].

For architectural purposes, openings are often required in SPSWs. There are two main ways to meet the needs of opening in current research and engineering practice, one is to directly arrange the door or window openings on the wall panel, the other is to apply beam-only-connected wall panels, that is, disconnect the wall panel from the boundary columns, so that not only the opening can be conveniently arranged, but also the pull-in forces from the wall panel on the columns can be eliminated. In addition, the wall panel connected with beams only are also convenient for designers to adjust the lateral stiffness and capacity of the structure by flexibly setting the span of wall panels.

Numerous experimental and numerical analyses have proved that openings on flat wall panels would reduce the lateral stiffness and capacity of the structure, but in most cases, it would improve the ductility of the structure to a certain extent [14,15]. Stiffeners at the opening edge could improve the performance to a certain extent [16,17]. In addition, absence of connections between the wall panel and boundary columns would lead to the partially development of TFA since that only part of TFA could be effectively anchored to boundary beams, which would significantly reduce the lateral stiffness, strength and energy consumption capacity of the structure [18,19]. Beam-only-connected wall panels were more likely to tear at the corners compared with four-side-connected panels, resulting in worse ductility [20]. Plate-edge restraint members could be used to alleviate the serious pinching of the hysteretic curve and reduction of lateral stiffness and strength of the SPSWs with beam-only-connected wall panels [18], and if the restraint members with sufficient rigidity and strength are used, TFA could be fully developed on the whole wall panel in theory, but such constraint members generally have large cross-section, which not only leads to high cost and complex construction, but also encroaches on part of the opening space [21].

As for CPSWs with openings, Farzampour et al. [22] conducted a numerical parametric study of the lateral behavior of vertical corrugated steel plate shear walls with a square opening and concluded that the ultimate strength of CPSWs with an opening could be calculated by multiplying the factor (1-d/D) based on the weakening of TFA development. In addition to hot-rolled steel shear walls, there were also some experimental studies of cold-formed steel (CFS) shear walls sheathed with corrugated sheet steel with openings [23, 24]. Different from hot-rolled steel shear walls, connector (fastener or screw) failure was the primary failure mechanism in conventional CFS shear walls, which resulted in a relatively low ductility compared to shear walls with panel yielding. In summary, existing investigations of SPSWs with openings on the wall panels are mainly based on TFA load-carrying mechanism of the wall panel, including the study of CPSWs with openings, and these few researches on the CPSWs structure with openings are numerical analysis rather than experimental study.

Considering that it is not convenient to manufacture openings in the middle of corrugated plates due to the special shape, the opening with the entire wallboard height is expected to be a feasible form to not only satisfy the architectural opening requirements but also have good seismic performance. Therefore, cyclic tests on corrugated steel plate shear walls with various infill panels (panel without opening, panel with bilateral gaps, panel with bilateral openings, and panel with central opening) were conducted to study the seismic performance of VCPSWs with various openings, and implication on seismic design was discussed.

2. Experimental program

2.1 Test specimens

As shown in Fig 1, a total of four specimens were designed and constructed to investigate the seismic performance of vertically corrugated steel plate shear walls (VCPSWs) with various infill panel designs. All the specimens were one-third-scale models with 2000mm wide and 2500mm high (1250mm of each story) and tested under cyclic quasi-static load. The configuration of the specimens are listed in Table 1. The parameters for this series of tests were the details of infill panels, including panel-frame connections forms (fully four-side-connected, beam-only-connected or three-side-connected), panel opening size (a small gap or door opening), and panel opening location (bilateral or central opening).

For all these four specimens, the wall panel thickness, the corrugation geometric properties of the infill corrugated wall panels, and the sizes of boundary frame members were the same. The thickness and steel material of the infill wall panels was 3mm and Q235 steel with a nominal yield strength of 235MPa, respectively. The corrugation geometric properties of the infill wall panel was designed to resist shear force by shear-yielding mechanism without elastic buckling according to Design Manual [25], that the shear buckling parameter λ_s which was determined according to reference [26], was smaller than 0.6. Corrugation shape is shown in Fig. 2.

The boundary frame members were built-up wide-flange sections, and in each specimen, the top-beam section and bottom-beam section had the same dimensions of H-300×200×14×16 (H - overall depth × flange width × web thickness × flange thickness, units: mm), the section of the middle-beam and the column was H-200×150×14×16 and H-200×200×14×16 respectively. The flange- and web-plates of all the beam and column sections satisfied the width-thickness limitations of current AISC seismic provisions [27]. It is helpful to further improve the seismic behavior of the structure under large inelastic deformations by preventing premature local buckling of columns [28].

For increasing the beam-column connection rotational ductility, the cover plate plus bolted double-angle moment connections were used in all the boundary frames, the connection details is shown in Fig.3. The cover plates were rigidly connected to the column flanges and beam flanges by full-penetration groove welds and three-sided filled welds, respectively. The beam webs were connected to column flange by bolted double-angle. Fig.3 also shows the details and differences of panel-frame connections in those four specimens. The infill panels were weld-connected to the boundary frame members using fishplates with 6mm thickness at flat edges and discrete steel angles at corrugated edges, respectively. In specimen S1, all the four edges of wall panels were weld-connected to the boundary frame members, as shown in Fig.1 (a). Infill wall panels of specimens S2 and S3 were welded only to the beams, as shown in Fig.1 (b) (c). Compared with specimen S2, the bilateral opening size of specimen S3 was much bigger, which could represent a normal door opening. Specimen S4 consisted two separated wall panels and an intermediate beam segment similar to coupling beam, which was more like a coupled SPSW system and formed a central opening whose width equal to total openings width of specimen S3, as shown in Fig.1 (d). In addition, for specimen S4, end plates with 100mm wide and 10mm thickness were welded to the free edges of infill wall panels at openings. Noted that the boundary beam and column sections were checked based on the capacity design method to prevent shear yielding of beam ends happening before the yielding of wall panels.

Steel used for the wall panels and boundary members was Q235 and Q345 with the nominal yield strength of 235MPa and 345MPa respectively. Material properties of steel members used in the specimens were evaluated through tensile coupon test. Three coupons were tested for each material. The average results of the coupon test are presented in Table 2.

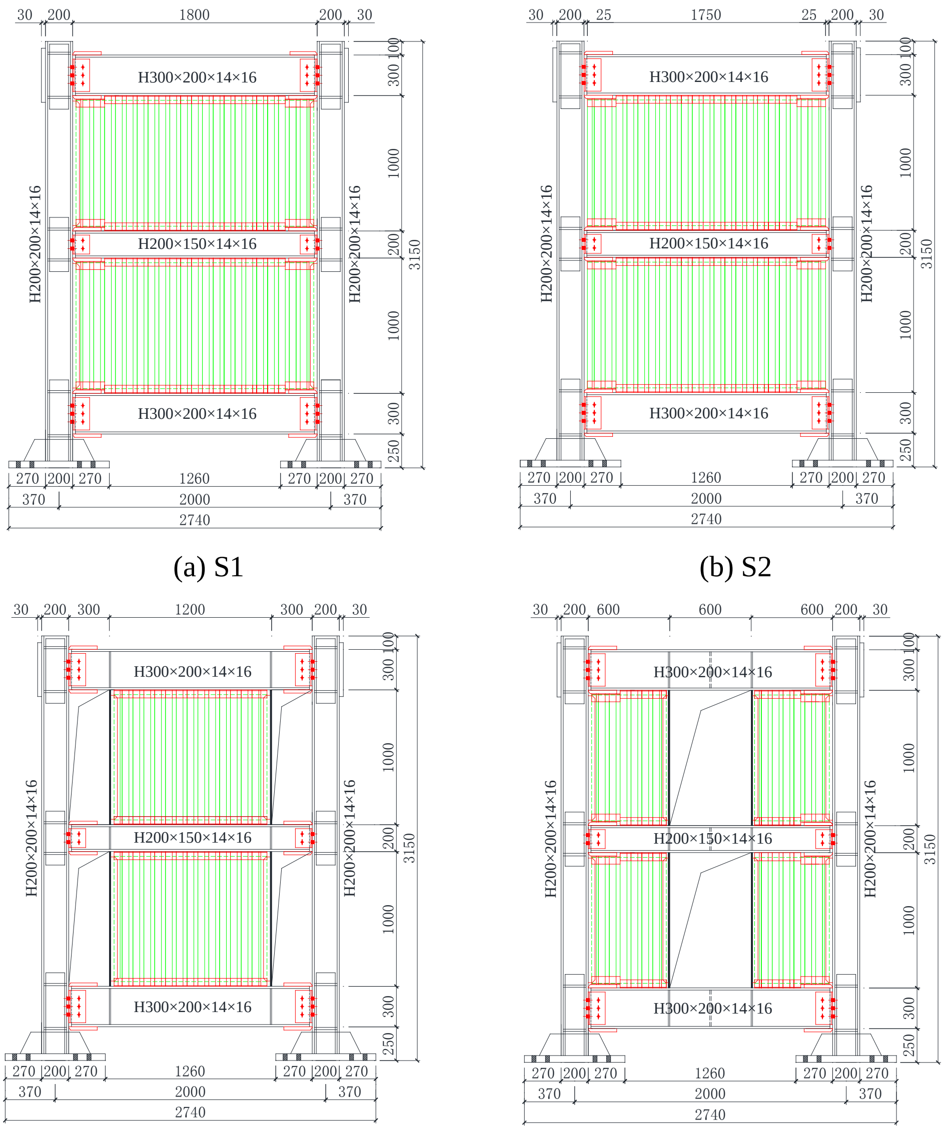

(a) S1 (b) S2

(c) S3 (d) S4

Fig. 1 – Specimens configurations (units: mm)

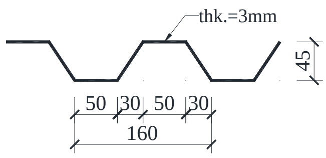

Fig. 2 – Shape of corrugation (units: mm)

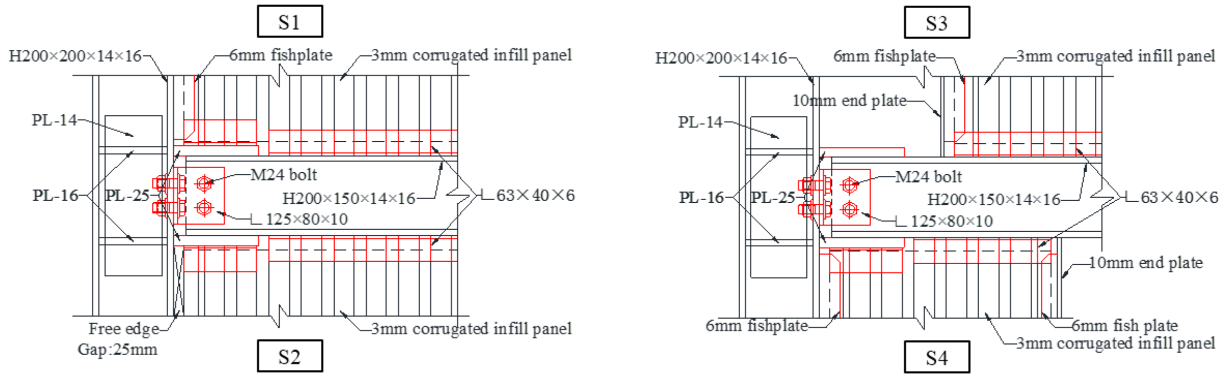

(a) S1 and S2 (b) S3 and S4

Fig 3. – Details of beam-to-column and panel-to-frame connection in different specimens

Table 1 – Test specimens

Specimens	Panel-frame connection	Panel opening location	Width of each opening (mm)	End plate on free edge
S1	Four-side-connected	Without openings	0	No
S2	Beam-only-connected	Bilateral gaps	25	No
S3	Beam-only-connected	Bilateral openings	300	Yes
S4	Three-side-connected	Central opening	600	Yes

Table 2 – Coupon test results

Member	Steel grade	Thickness (mm)		Elastic modulus (GPa)	Yield stress (MPa)	Ultimate stress (MPa)	Elongation at rupture (%)
		Nominal	Actual				
Wall panel	Q235	3	3.0	193.3	312.3	451.3	39.4
Fish plate	Q235	6	5.7	204.3	336.0	460.0	36.9
End plate	Q235	10	9.6	196.7	345.0	/	/
Web plate	Q345	14	14.0	202.6	357.3	513.3	34.6
Flange plate	Q345	16	16.6	183.5	334.8	468.9	34.1
Note: / means invalid data.							

2.2 Test setup, instrumentations, and load procedures

A photograph of the test setup is shown in Fig.4 (a). The specimen was oriented in the East-West direction, and lateral load was applied quasi-statically to the top-beam end though a hydraulic actuator with the maximum ability of 3200kN, which was supported by a reaction wall. The specimen was fixed to a base beam attached to the strong floor. To prevent the out-of-plane deflection of the specimen, lateral support was provided to the region of column near the top-beam.

A number of linear variable displacement transduces (LVDTs) were put on the specimens to measure the global as well as local displacements of points of interest on the specimens. Taking specimen S1 for example, Fig. 4(b) illustrates the arrangement of LVDTs. Three LVDTs were arranged along the centerlines of all the beams, two LVDTs were arranged at the above and below of middle-beam's ends, four LVDTs were arranged along the diagonal lines of infill panels, and four LVDTs were arranged at the base plates of the specimen and the base beam. In this way, movements of the members and sliding deformation of the specimen relative to the base beam and the strong floor were monitored, and important date such as shear deformation of the infill panel, and rotation of beam-column connection could be measured.

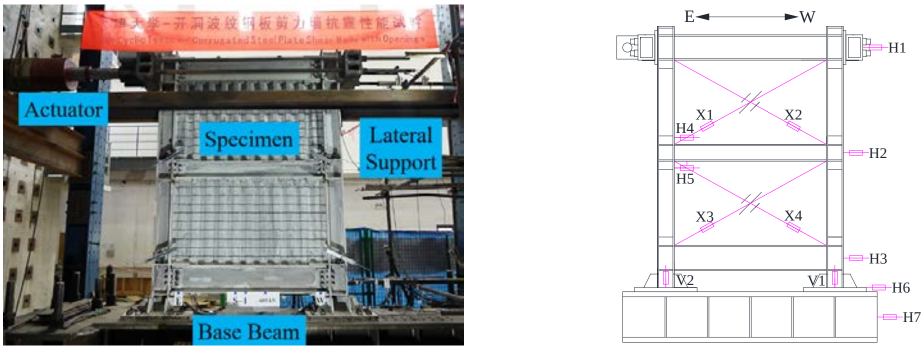

(a) Test setup (b) Arrangement of LVDTs

Fig 4. – Test setup and LVDTs Arrangement

Linear and rosette strain gauges were mounted to the specimens, as shown in Fig.5. The arrangement of strain gauges at the boundary frame was the same for all the specimens, while the arrangement at the infill panels was somewhat different for each specimen. Each specimen was completely painted using whitewashes and a grid pattern was left on the wall panel to provide a good visual indicator of the specimen behavior. The location where the plastic deformation developed could be recognized by observing the whitewash flaking.

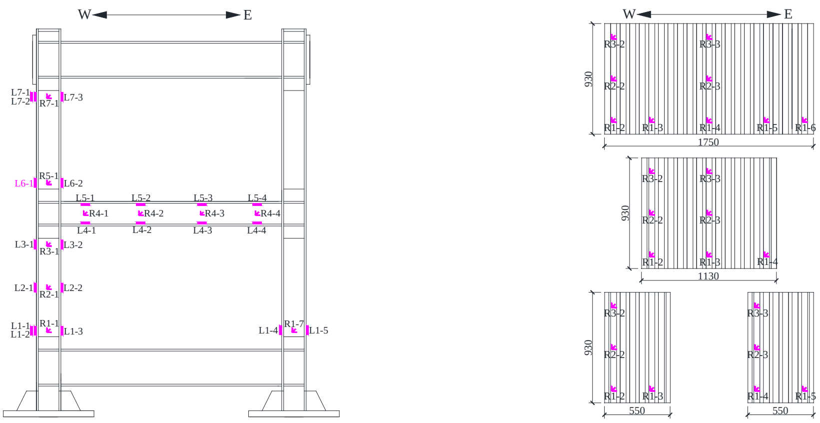

(a) Boundary members (b) Infill wall panels

Fig 5. – Arrangement of strain gauges at specimens

The lateral loads were imposed using the combination of the force-control scheme and displacement-control scheme, as shown in Fig. 6.

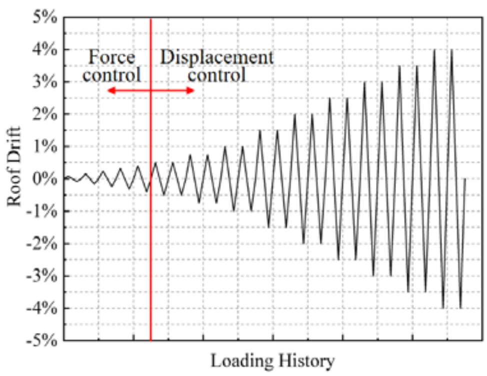

Fig 6. – Loading protocol

3. Experimental results

Fig. 7 shows the lateral force verses total structural drift relationships obtained from the test results of the four specimens. It's worth noting that the total structural drift was determined through the relative displacement between the top-beam and below-beam, and was a little different from the roof drift used for loading control. It could be seen in the figure that all four specimens showed good hysteretic behavior with the hysteretic curves full without pinching.

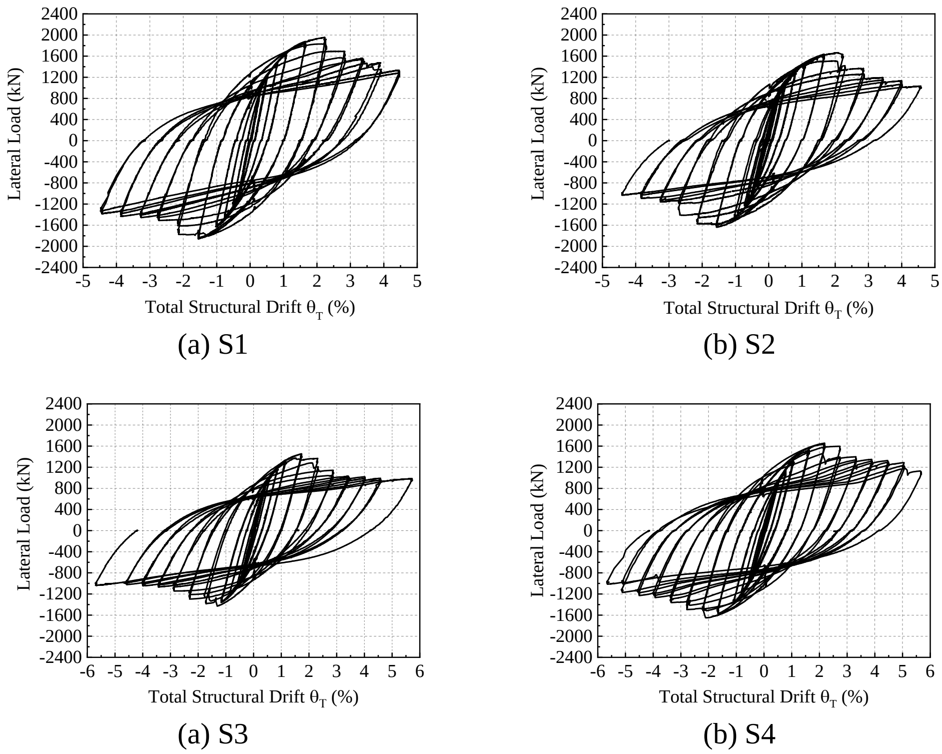

Fig 7. – Experimental cyclic lateral force versus total structural drift relationships

Fig. 8 shows the typical failure pattern of each specimen after the cyclic test. Combining the detailed experimental observations during loading of each specimen, it could be found that all specimens experienced basically similar failure process, that is, infill wall panels yielded at about 0.5% drift, causing slightly expansion of the hysteresis loops, which could be regarded as the structural yielding; then the middle beam and the columns developed plasticity gradually; afterwards, the plastic deformation of the corrugated wall panel started to occur at about 1.5%-2% lateral drift; connections between the column flange and the beam flange began to fail at about 2% lateral drift, which were caused by the fracture of the full-penetration butt weld between the column flange and cover plate at the middle beam; eventually, as the deformation and cracks on the panel as well as the deformation at the beam end and column bottom became more severe, the bearing capacity of the specimen decreased gradually until they failed at a relatively large lateral drift of 4%-5%.

Deformation of corrugated wall panels in these specimens did not cause loud noise and sudden decrease of the lateral capacity. Moreover, the reduction of bearing capacity caused by further deformation and scattered tearing of the corrugated wall panel was relatively slow. However, all specimens experienced the unexpected cracking of the weld between the flange cover plate at the middle beam end and the column flange, which might be mainly due to the deficient weld processing quality and insufficient consideration of the deformation capacity of the connection in the specimen design. It should be noted that the drift was relatively large when the beam end fracture occurred, and the infill wall panel, middle beam and columns had developed plasticity, so in fact, such immature failure had little impact on the ultimate bearing capacity of the specimen, but the ductility of the specimen had been evidently reduced due to the sudden drop of bearing capacity.

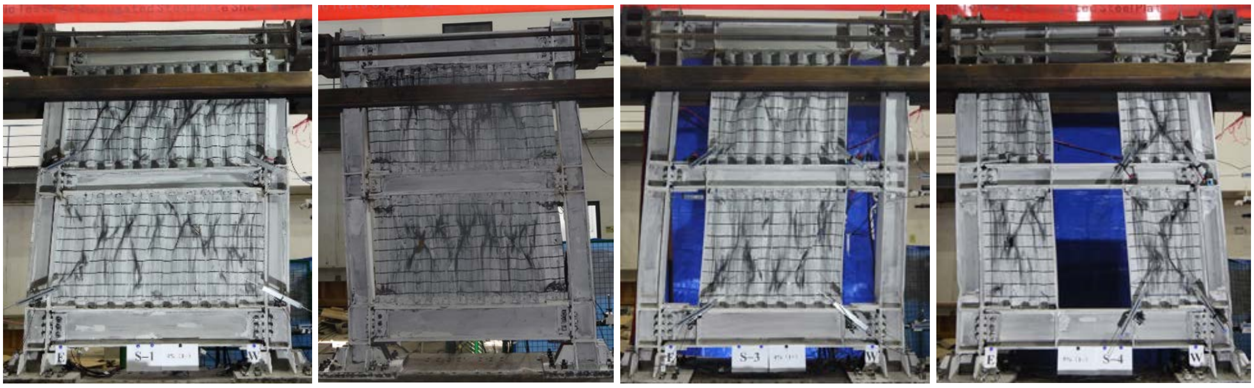

(a) S1 (b) S2 (c) S3 (d) S4

Fig 8. – Deformation pattern of specimens at the end of testing

3.1 Lateral stiffness and capacity

Lateral load-total structural drift skeleton curves and stiffness curves of all these four specimens are shown in Fig. 9 (a) and (b) respectively. All the specimens exhibit three loading stages, that is, elastic stage, elastic-plastic stage and descent stage. In addition, there is an obvious turning point on the skeleton curve of each specimen due to shear-yielding of infill panels.

The initial stiffness and ultimate capacity of specimen S1 were higher than those of other three specimens. The main reason could be the largest width of infill panel and the fully panel-frame connections in this specimen. The initial stiffness and ultimate load-resisting capacity of specimen S2, whose infill panels width were almost the same with specimen S1, were 20.4% and 13.3% less than those of specimen S1 respectively. This indicated that corrugated steel plate shear walls with bilateral gaps still have a good lateral-resisting performance, but the reduction in initial stiffness and lateral load-resisting capacity should be considered in the design. As for specimen S3 and specimen S4, although the width of infill wall panels were the same with the opening ratio of 33%, the initial stiffness and load-resisting capacity of these two specimens were different. Compared with specimen S1 without openings, the initial stiffness of specimen S3 and specimen S4 were reduced by 27.0% and 32.8%, and the lateral load-resisting capacity were reduced by 25.5% and 13.7%, respectively. It indicated that different opening location had a different influence on the structural behavior. Meanwhile, although the total infill panel width of specimen S4 was 30% smaller than that of specimen S2, their ultimate capacity were almost the same, this was mainly because of the end plates welded to the free edges of corrugated infill panels of specimen S4 could improve the load-carrying capacity efficiency of corrugated infill panels.

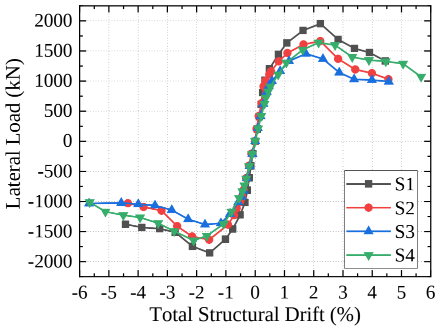

(a) Lateral capacity vs. total structural drift

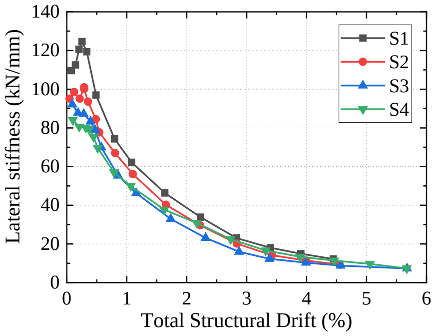

(b) Lateral stiffness vs. total structural drift

Fig 9. – Skeleton curves of lateral capacity and stiffness

3.2 Ductility and energy consumption

Deformability and energy dissipating capacity under seismic load are major parameters of lateral load-resisting systems. The ductility ratio of each test specimen is summarized in Table 3. The yield valves used to calculate ductility ratio were determined based on ATC-24, associated with significant yielding in critical region of the test specimens which were reflected by a clear nonlinearity in the force-deformation relationship. The ductility of the test specimens were in range of 4.67-6.12, which exhibited good deformation capacity. Specimen S1 without openings had the highest ductility among the test specimens, while specimen S4 with central opening had the lowest ductility. The difference of ductility mainly came from the difference of immature failure at the beam end, which indirectly reflects the requirements of rotation capacity of the joint. Therefore, for the corrugated steel plate shear walls, bilateral gaps or bilateral openings increased the rotational demand of the beam-column connection, and connection forms with higher rotational capacity might need to be considered in the future.

Table 3 – Summary of test results

Specimens	Initial Stiffness (kN/mm)	P_y (kN)	θ_y (%)	P_m (kN)	θ_m (%)	θ_u (%)	Ductility ratio θ_u / θ_y
S1	119.4	1214	0.50	1905	1.90	2.75	5.53
S2	95.0	1059	0.50	1651	1.90	2.73	5.46
S3	87.2	1007	0.58	1420	1.73	2.69	4.67
S4	80.2	927	0.54	1644	2.14	3.27	6.12

Note: all the data were the average value of both positive and negative loading direction results. P_y = yield load; θ_y = yield total structural drift; P_m = peak lateral capacity; θ_m = total structural drift at P_m; and θ_u = total structural drift when the capacity dropped to 85% of its peak capacity.

As illustrated in Fig. 7, all the specimens dissipated energy with stable and plump hysteresis loops, which exhibited excellent energy consumption capacity, and it was different with the fact that pinching hysteresis loops were commonly observed in the SPSWs with flat infill panels. Fig. 10 shows the cumulated energy consumption of test specimens. At the same total structural drift, the energy dissipation capacity of specimen S2, whose infill wall panels connect with beams only, was less than that of specimen S1, whose infill panels connected with beams and columns. This is because that the effective load-carrying and energy consumption area of the infill panel reduced due to the disconnection between infill panel and column. Similarly, the dissipation capacity of specimen S3 and specimen S4 were decreased by the opening on the wall panel. Compared with specimen S1 without opening, at about 4% drift, the cumulative energy dissipations of specimens S2, S3 and S4 were reduced by 16.2%, 24.3% and 15.6%, respectively.

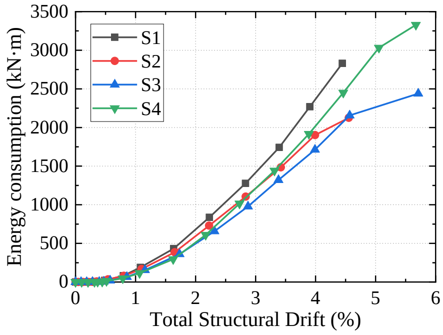

Fig 10. – Cumulative energy consumption of test specimens

3.3 Strain development of infill wall panels

Fig. 11 shows the shear strain at various positions on the wall panel of each specimen. It can be seen from the figure that when the lateral drift of the test specimens reached the yield drift θ_y, which was listed in Table

3, the shear strain at each position on the wall panel had been above the material shear yield strain value, which means that most area of the wall panel had been in the state of shear yielding, indicating that the value of yield drift was reasonable. Specifically, in the elastic stage, the shear strain value is basically linear with the lateral drift, and the strain values at different positions of the specimen are basically the same, indicating that the shear deformation of the wall panel is relatively uniform; when the shear strain value exceeds the material shear yield strain value, the shear strain value at most positions increases rapidly. Combined with the observation that the lateral drift when the deformation of the corrugated wall panels started to occur was about 1.5%-2% lateral drift, it could be seen that the corrugated wall panel in these specimens did not show elastic buckling, but experienced plastic deformation.

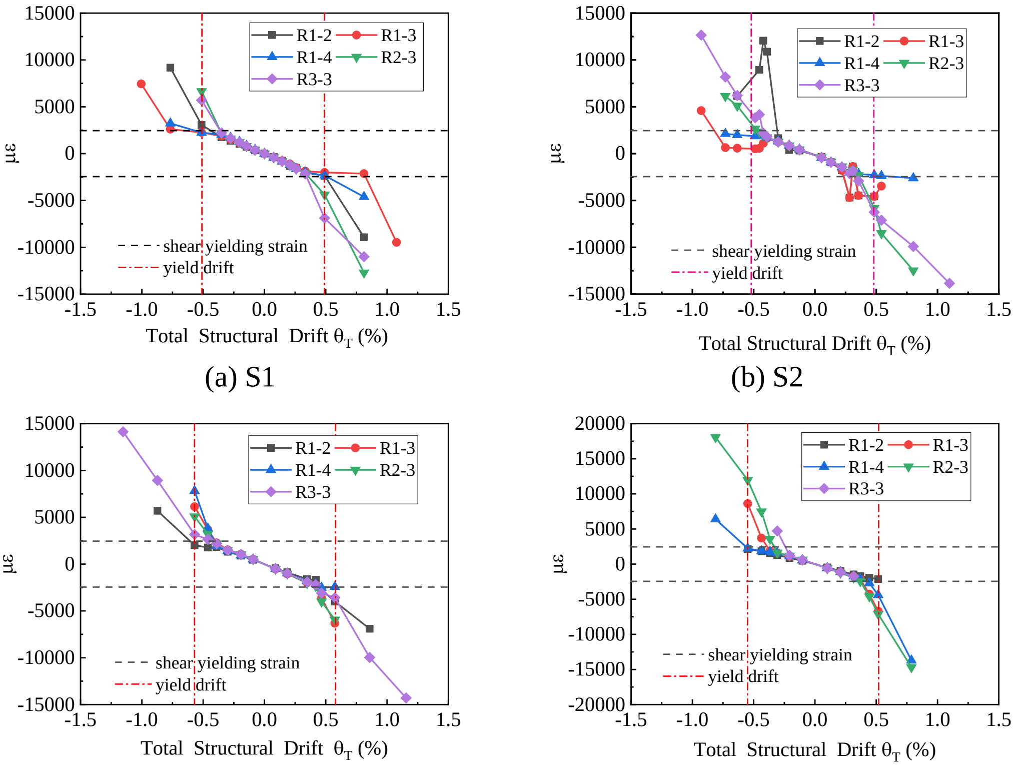

(a) S1 (b) S2

(a) S3 (b) S4

Fig 11. – Shear strain development of infill wall panels

4. Conclusion

A total of four cyclic tests were conducted to investigate the seismic behavior of the vertical corrugated steel plate shear walls (VCPSWs) with various infill panels (panel without opening, panel with bilateral gaps, panel with bilateral openings, and panel with central opening). Failure mode, cyclic behavior, strength and stiffness properties, deformation and energy dissipation capacities of the specimens were presented and discussed. Influences of opening size, opening location and end plates at the free edges on system seismic behavior were studied. The main conclusions are as follows:

(1) All four specimens showed good seismic performance with high lateral stiffness, lateral capacity, ductility and energy dissipation capacity. All specimens experienced basically similar failure process that the infill wall panel yielded and dissipated energy at about 0.5% drift firstly, then the boundary frame beams and columns developed plasticity gradually. As the deformation and cracks on the panel as well as the deformation at the beam end and column bottom became more severe, the capacity of the specimen decreased gradually until they failed at a relatively large lateral drift of 4%-5%.

(2) Corrugated wall panels in these specimens did not show elastic buckling, but experienced plastic deformation, which did not cause loud noise or sudden decrease of the bearing capacity.

(3) Vertical corrugated steel plate shear wall with bilateral gaps, bilateral openings and central opening all had considerably reduced lateral capacity, stiffness and cumulated energy consumption capacity, compared with the specimen with no opening. The lateral bearing capacity were reduced by 13%, 26%, 14% respectively, for specimen with bilateral gaps, bilateral openings and central opening , while the lateral stiffness were reduced by 20%, 27%, 33% respectively. With the same opening ratio, the lateral stiffness of the specimen with bilateral openings was 8% lower than the specimen with central opening, but with higher capacity and ductility, which might be mainly due to the immature beam-column connections failure in the former.

(4) Welding end plates to the free edges of corrugated wall panels improved the load-carrying efficiency evidently. For the corrugated steel plate shear walls, bilateral gaps or bilateral openings increased the rotational demand of the beam-column connection, and connection forms with higher rotational capacity might need to be considered in the future.

5. Acknowledgements

The authors of this paper would like to express their appreciation for the financial support given by the National Natural Science Foundation of China (No. 51378340, 51678406 and 51878447). Support from the funding agency above is gratefully acknowledged.

6. References

[1] Astaneh-Asl A (2001) Seismic behavior and design of steel plate shear walls. *2001 SEOANC Seminar. San Francisco: Structural Engineers Association of Northern California*, San Francisco, USA.

[2] Mathias N, Sarkisian M, Long E, Huang Z (2008): Steel plate shear walls: Efficient structural solution for slender high-rise in China. *Seismic Engineering Conf. Commemorating the 1908 Messina and Reggio Calabria Earthquake*, Reggio Calabria, Italy.

[3] Berman JW (2011): Seismic behavior of code designed steel plate shear walls. *Engineering Structures*, **33** (1), 230-244.

[4] Berman JW, Bruneau M (2005): Experimental investigation of light-gauge steel plate shear walls. *Journal of Structural Engineering*, **131**, 259-267.

[5] Emami F, Mofid M, Vafai A (2013): Experimental study on cyclic behavior of trapezoidally corrugated steel shear walls. *Engineering Structures*, **48**, 750-762.

[6] Zhao Q, Sun J, Li Y, Li Z (2017): Cyclic analyses of corrugated steel plate shear walls. *Structural Design of Tall and Special Buildings*, **26** (16), e1351.

[7] Qiu J, Zhao Q, Yu C, Z Li (2018): Experimental studies on cyclic behavior of corrugated steel plate shear walls. *Journal of Structural Engineering*, **2144** (11), 04018200.

[8] Hosseinzadeh L, Emami F, Mofid M (2017): Experimental investigation on the behavior of corrugated steel shear wall subjected to the different angle of trapezoidal plate. *Structural Design of Tall and Special Buildings*, **26** (17), e1390.

[9] Cao Q, Huang J (2018): Experimental study and numerical simulation of corrugated steel plate shear walls subjected to cyclic loads. *Thin-Walled Structures*, **127**, 306-317.

[10] Kalali H, Hajsadeghi M, Zirakian T, Alaee FJ (2015): Hysteretic performance of SPSWs with trapezoidally horizontal corrugated web-plates. *Steel Composite Structures*, **19** (2), 277-292.

[11] Dou C, Pi YL, Gao W (2018): Shear resistance and post-buckling behavior of corrugated panels in steel plate shear walls. *Thin-Walled Structures*, **131**, 816-826.

[12] Dou C, Jiang ZQ, Pi YL, Guo YL (2016): Elastic shear buckling of sinusoidally corrugated steel plate shear wall. *Engineering Structures*, **121**, 136-146.

[13] Zhao Q, Li Y, Sun J. (2017): Analyses on seismic behavior of corrugated steel plate shear walls. *Annual Stability Conference Structural Stability Research Council*, San Antonio, Texas, USA.

[14] Pellegrino C, Maiorana E, Modena C (2009): Linear and non-linear behaviour of steel plates with circular and rectangular holes under shear loading. *Thin-Walled Structures*, **47** (6), 607-616.

[15] Afshari MJ, Gholhaki M (2018): Shear strength degradation of steel plate shear walls with optional located opening. *Archives of Civil and Mechanical Engineering*, **18** (4), 1547-1561.

[16] Hosseinzadeh SAA, Tehranizadeh M (2012): Introduction of stiffened large rectangular openings in steel plate shear walls. *Journal of Constructional Steel Research*, **77** (10), 180-192.

[17] Nie JG, Zhu L, Fan JS, Mo YL (2013): Lateral resistance capacity of stiffened steel plate shear walls. *Thin-Walled Structures*, **67** (2), 155-167.

[18] Choi IR, Park HG (2009): Steel plate shear walls with various infill plate designs. *Journal of Structural Engineering*, **135** (7), 785-796.

[19] Clayton PM (2013): *Self-centering steel plate shear walls: subassembly and full-scale testing*. Ph.D. Dissertation, University of Washington.

[20] Vatansever C, Yardimci N (2011): Experimental investigation of thin steel plate shear walls with different infill-to-boundary frame connections. *Steel and Composite Structures*, **11** (3), 251-271.

[21] Hou J (2016): *Hysteretic behavior of steel plate shear wall and buckling restrained steel plate shear wall with side columns*. M.S. Thesis, Fuzhou University. (in Chinese)

[22] Farzampour A, Laman JA, Mofid M (2015): Behavior prediction of corrugated steel plate shear walls with openings. *Journal of Constructional Steel Research*, **114**, 258-268.

[23] Yu C, Yu GW (2016): Experimental investigation of cold-formed steel framed shear wall using corrugated steel sheathing with circular holes. *Journal of Structural Engineering*, **142** (2), 04016126.

[24] Dai XM, Ding Y, Zong L, Deng EF, Lou N, Chen Y (2018) Experimental study on seismic behavior of steel strip reinforced CSPSWs in MBS. *Journal of Constructional Steel Research*, **151**, 228-237.

[25] Japan Society of Civil Engineers (1998): *Design manual for PC bridges with corrugated steel webs*. Research Committee for Hybrid Structure with Corrugated Steel Webs, Japan Society of Civil Engineers, Tokyo. (in Japanese)

[26] Yi J, Gil H, Youm K, Lee H (2008): Interactive shear buckling behavior of trapezoidally corrugated steel webs. *Engineering Structures*, **30** (6), 1659-1666.

[27] American Institute of Steel Construction (2016): *Seismic provisions for structural steel buildings*. ANSI/AISC 341-16, Chicago, USA.

[28] Park HG, Kwack JH, Jeon SW, Kim WK (2007): Framed steel plate wall behavior under cyclic lateral loading. *Journal of Structural Engineering*, **133** (3), 378-388.

